# ACCURATE CALIBRATION OF DOPPLER WINDS FOR THEIR USE IN THE COMPUTATION OF MESOSCALE WIND FIELDS [1]

TETSUYA FUJITA

Department of the Geophysical Sciences, The University of Chicago, Chicago, Ill.

## ABSTRACT

Doppler winds measured by an instrumented aircraft are of great value in determining the wind field accompanying large-scale atmospheric disturbances. When they are utilized in interpreting and computing the wind fields of so-called mesoscale disturbances with their horizontal dimensions of a few to a few hundred miles, slight errors in the vector quantities forming the navigation triangle result in fictitious winds which differ considerably from the real winds. In the first part of this paper, the wind velocity errors due to the backscattering water particles illuminated by Doppler beams, designated as wet beams, are discussed. The influence of wet beams upon Doppler winds was calculated theoretically under various conditions to allow an estimate of maximum wind velocity error. Following the solution of wet-beam cases, theoretical consideration was given to the fluctuation of the measured winds caused by the constant errors in the true air speed, the aircraft heading, the Doppler ground speed, and the Doppler drift angle. For the purpose of investigating whether this type of error occurs or not, test flights were made over Florida and Oklahoma along a number of loops with varying diameters. Results of the evaluation revealed that the error in aircraft heading is of least importance and that the other errors can be determined and corrected with a high degree of accuracy provided only a few specific loops are flown during each mission. It has become feasible to calculate both divergence and vorticity associated with mesoscale disturbances from the calibrated Doppler winds measured along well-designed flight tracks. It is expected that the basic research presented in this paper will stimulate the use of Doppler wind systems in the determination of the detailed structure of winds accompanying mesoscale meteorological systems.

## 1. INTRODUCTION

During the past 10 years or more, airborne Doppler wind systems have been used in meteorology for both research and operational purposes. Doppler winds measured along aircraft tracks at flight levels give much higher horizontal space resolution than could be expected from existing upper-air networks.

In an attempt to study the structure of hurricanes, which had previously been described only by fortunate soundings that went through specific portions of the storms, Simpson [9] utilized Doppler winds obtained on a special mission by the Air Weather Service of the U.S. Air Force. Both the frequency and the accuracy of the winds used in his pioneering work were inferior to those available now; nevertheless, the significant results he obtained paved the way for the utilization of Doppler winds in research on hurricanes using specially instrumented aircraft. The wind data obtained by the National Hurricane Research Project (NHRP) and later by the Research Flight Facility (RFF) research aircraft have been used successfully by many hurricane researchers, including LaSeur and Hawkins [6], who recently investigated the three-level wind structure of hurricane Cleo. It has been recognized through these studies that Doppler winds are quite representative of the wind fields of storms as a whole, which can be described effectively by plotting winds on the coordinates moving with each storm.

When Doppler winds are used to reveal the wind fields associated with small but violent systems, such as thunderstorms and squall lines or precipitation cells within the hurricane rainband, the basic problem of the representativeness and accuracy of the winds needs to be fully investigated.

Under the strong turbulence associated with a squall line, an Air Force B–47 equipped with an AN/APN–66 Doppler system measured winds at about 38,000 ft. over Texas. An analysis of this storm by McLean [7] revealed the existence of a divergent flow superimposed upon the mean gradient wind at that level. An outflow of extremely large magnitude and of similar pattern (Arnett [1]) was observed at 39,000 ft. over a cluster of thunderstorms southeast of Oklahoma City. An increase in winds from upwind of 80 kt. to downwind of 120 kt. would result in a divergence, $46 \times 10^{-5}$ sec.$^{-1}$ which is comparable to that of a surface divergence accompanied by an intense mesohigh.

Three-level wind data obtained by RFF aircraft flying around and over an isolated cumulonimbus were analyzed by Fujita and Arnold [4]; this led to the description of the low-level convergence, the middle-level flow which

[1] The research reported in this paper has been supported by the National Severe Storms Project, U.S. Weather Bureau, under grant Cwb WBG-20, and partially by the National Severe Storms Laboratory, U.S. Weather Bureau, under grant Cwb WBG-41. The photogrammetric portion of this paper is sponsored by the National Science Foundation under grant NSF G 18984.

goes around the convective cell, and the diverging flow above the cloud top. The results thus obtained seem to fit the general picture of an isolated storm which might be imagined from one's existing knowledge. It is, however, rather difficult to discover from Doppler winds an unknown field of motion around a cloud unless it can be expected from existing theory or fits a model established by a researcher. When a peculiar wind field appears within a small area, it might well be smoothed out on the assumption that it is a consequence of some errors in the Doppler wind system.

Basic problems in the use of Doppler winds are closely related to the scales and nature of the meteorological disturbances to be investigated. Airborne Doppler wind and navigation systems would perform with extreme accuracy if a flight were made along a more or less straight line over cloud-free regions. Such a flight would be satisfactory for commercial airlines, but a research flight requires frequent turns and cloud penetrations which naturally interfere with accurate measurements of winds by a Doppler system. It is the purpose of this paper to estimate such errors and to try to eliminate them as much as possible before a mesoscale analysis of detailed wind fields is attempted.

### BASIC SYMBOLS AND DEFINITIONS

For the purpose of identifying various quantities used in this paper, a brief summary of the basic symbols and definitions is presented.

HORIZONTAL VELOCITY. The horizontal component of a three-dimensional velocity vector with respect to the earth's surface is identified by a bold letter. This velocity should be correctly called the horizontal ground velocity, but the term "ground" is omitted in this paper.

**D**, termed "effective Doppler velocity," is expressed by $\mathbf{D}=\mathbf{G}-\overline{\mathbf{T}}$

$\mathbf{D}_0$, measured by Doppler system, termed "Doppler velocity"

**G**, of aircraft, i.e., "ground velocity"

**M**, of moving water surface, i.e., ocean, lake, river

**R**, of raindrops

**S**, of spray

**V**, of any backscattering objects

**W**, of wind, i.e., wind velocity

VERTICAL VELOCITY. The vertical component of a three-dimensional velocity vector with respect to the earth's surface.

**G'**, of aircraft. Positive values upward

**R'**, of falling raindrops, termed "fall velocity." Positive values downward

EFFECTIVE VELOCITY. A fraction of the horizontal velocity contributing to the frequency shift measured by a specific beam. This term should be correctly called the effective horizontal velocity, but the term "horizontal" is omitted in this paper.

$\overline{\mathbf{M}}=k_M\mathbf{M}$, $\overline{\mathbf{R}}=k_R\mathbf{R}$, $\overline{\mathbf{S}}=k_S\mathbf{S}$, and $\overline{\mathbf{V}}=k_V\mathbf{V}$.

$\overline{\mathbf{T}}=\Sigma\overline{\mathbf{V}}=\overline{\mathbf{M}}+\overline{\mathbf{R}}+\overline{\mathbf{S}}$ is termed the "total effective velocity."

$\mathbf{D}=\mathbf{G}-\overline{\mathbf{T}}$ denotes the effective Doppler velocity.

EFFECTIVE VERTICAL VELOCITY. A fraction of the vertical velocity contributing to the frequency shift measured by a specific beam. This is expressed by adding a prime to the symbol for horizontal velocity.

$\overline{\mathbf{R}}'=k_R'\mathbf{R}'$ and $\overline{\mathbf{V}}'=k_V'\mathbf{V}'$.

HORIZONTAL SPEED. The absolute value of a horizontal velocity vector. The capital italic letter corresponding to the bold capital designating a specific horizontal velocity is used.

$D$ for $\mathbf{D}$, $D_0$ for $\mathbf{D}_0$, . . ., etc.

VERTICAL SPEED. The absolute value of a vertical velocity vector. This is expressed by adding a prime to the symbol for horizontal speed.

$G'$ for $G$ and $R'$ for $R$.

AZIMUTH OF HORIZONTAL VELOCITY. The azimuth of a horizontal velocity vector translated to the sub-aircraft point. The azimuth is expressed by the small italic letter corresponding to the capital italic letter designating a specific horizontal speed.

$d$ for $D$, $d_0$ for $D_0$, $g$ for $G$, $m$ for $M$, $r$ for $R$, $t$ for $T$, $v$ for $V$, and $w$ for $W$.

ANGLES DESIGNATING BEAM ORIENTATION.

$\eta_0$ beam nadir angle: nadir angle of the beam which is kept constant by the vertical stabilization system.

$\psi_0$ beam horizontal angle: the horizontal angle between the beam and the direction of Doppler velocity. This angle is also constant for each Doppler system.

$\alpha$ azimuth of the beam.

## 2. FREQUENCY SHIFT FOR A SINGLE DOPPLER BEAM

Under the assumption that the motions of the airplane and the backscattering mediums are restricted to a vertical plane including a Doppler beam with its nadir angle $\eta_0$, the frequency shift can be expressed by

$$\Delta\nu=\frac{2\nu_0}{c}\{(G-\overline{R}-\overline{S}-\overline{M})\sin\eta_0-(G'+\overline{R}')\cos\eta_0\}, \quad (1)$$

where $\nu_0$ denotes the transmitted frequency and $c$, the speed of the electromagnetic wave of the Doppler system. The quantities $G$, $R$, $S$, and $M$ represent, respectively, the horizontal speed of the aircraft, raindrops, sea spray, and moving water surface (see fig. 1). The term including the vertical speed of the aircraft, $G'$, and the fall speed of raindrops, $R'$, should be added whenever necessary. Because of a limited amount of energy backscattered by raindrops, spray, and the water surface, a coefficient[2] $k$ must be multiplied by each of the horizontal speeds except $G$, thus

$$\overline{R}=k_RR,\ \overline{S}=k_SS, \text{ and } \overline{M}=k_MM. \quad (2)$$

[2] Edwin Kessler introduced in his unpublished manuscript "Report Concerning Test Flight With APS-20B Radar and Its Suggested Uses for Hurricane and Thunderstorm Reconnaissance," a similar coefficient which is to be multiplied by wind velocities to obtain sea-surface movement contributing to measured Doppler velocities. (The Travelers Research Center, Inc., Report, Jan. 1962.)

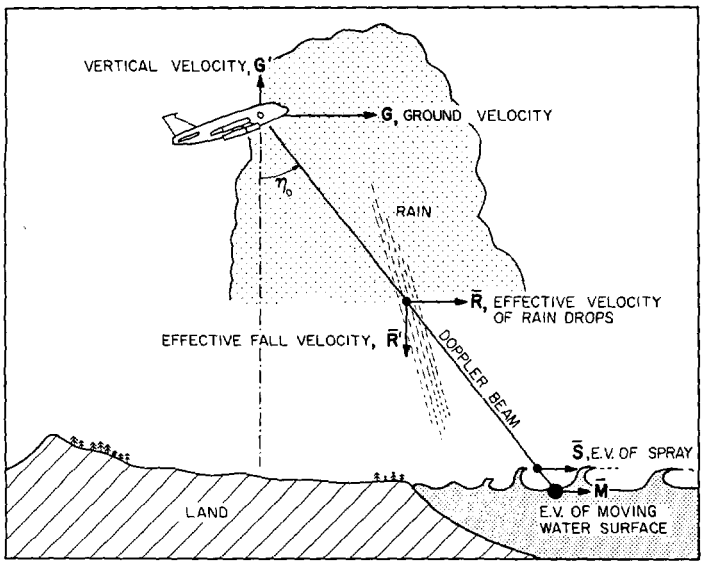


FIGURE 1.—Showing meteorological causes affecting the frequency shift measured by a single beam. Besides the ground velocity of the aircraft, the motion of falling raindrops, sea spray, and the moving water surface affect the frequency shift to a certain extent determined by the nature of the moving objects and the modes of frequency shift determination.

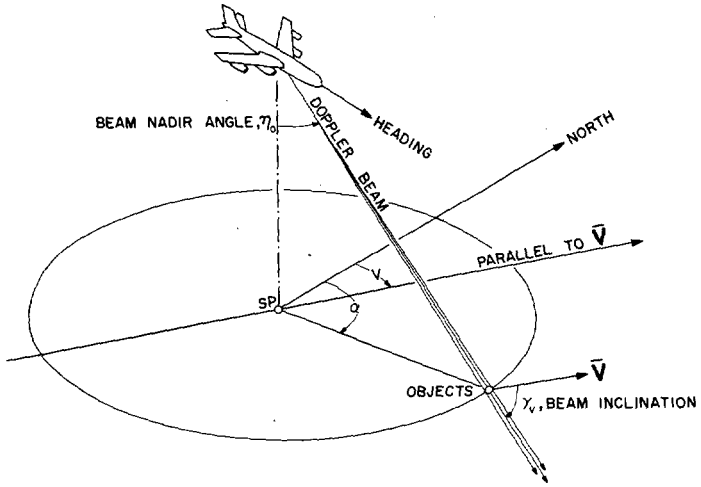


FIGURE 2.—Three-dimensional vectorial relationship between a Doppler beam and the velocity of moving objects illuminated by the beam. The frequency shift is proportional to the cosine of the beam inclination multiplied by the effective speed of the objects. Effective velocity $\bar{V}$ is defined as $k\mathbf{V}$, where $k$ represents a fraction of the total velocity which contributes to the frequency shift.

The sum of these coefficients should always be expressed by

$$k_R+k_S+k_M=1. \tag{3}$$

It should be noted that these coefficients vary, not only as a result of the backscattering characteristics of the mediums but also according to the type of the frequency-measuring devices. Some frequency trackers measure the shift of the frequency of the maximum return signal, while others compute the mean frequency. It is evident that fast-moving particles with low return signal do not alter the frequency of the maximum return signal, but the mean return frequency could be appreciably changed. A specific frequency-measuring element such as the frequency discriminator as discussed by Berger [2] determines the frequency shift when the signal intensities of the wings on both sides of the maximum return signal become identical. The frequency shift thus obtained is greatly influenced by the return signals from fast- and slow-moving objects.

Equation (3) indicates that the horizontal speed contributing to the Doppler shift is always smaller than the mean speed of the moving objects. This speed

$$\bar{V}=kV$$

is called the "effective speed" and is applicable to any volume of moving objects illuminated by a specific beam.

## EQUATION OF PARTIAL DOPPLER SHIFT MEASURED BY A SINGLE BEAM

We shall now obtain the equation to calculate the Doppler frequency shift caused by horizontally moving objects with the effective velocity $\bar{V}$ oriented in any direction (see fig. 2). The partial contribution of this effective velocity to the total Doppler shift for a beam is independent of the aircraft velocity and is expressed by

$$\delta\nu_V=-\frac{2\nu_0}{c}\bar{V}\cos\gamma_V, \tag{4}$$

where $\gamma_V$ is the "beam inclination", the direction of the beam measured from the effective velocity, $\bar{V}$. Expressing azimuths of the beam and the effective velocity translated to the sub-aircraft point by $\alpha$ and $v$, respectively, we write

$$\cos\gamma_V=\sin\eta_0\cos(\alpha-v),$$

which is put into equation (4) to obtain

$$\delta\nu_V=-\frac{2\nu_0\sin\eta_0}{c}\bar{V}\cos(\alpha-v)$$

$$=-C_0\bar{V}\cos(v-\alpha), \tag{5}$$

where $C_0=2\nu_0c^{-1}\sin\eta_0$ is a constant as long as the beam nadir angle is kept constant. With the use of a complex variable, equation (5) is now expressed by the real part of an exponential function,

$$\delta\nu_V=-C_0\bar{V}e^{i(v-\alpha)}. \tag{6}$$

## EQUATION OF TOTAL DOPPLER SHIFT FOR A SINGLE BEAM

In order to obtain the total frequency shift for a single beam caused by horizontal velocities, it is necessary to add together all partial shifts due to the ground speed of the aircraft, raindrops, sea spray, moving water surface, and other causes if existing. Thus

$$\Delta\nu=\delta\nu_G+\delta\nu_R+\delta\nu_S+\delta\nu_M$$

$$=C_0\{Ge^{i(g-\alpha)}-\bar{R}e^{i(r-\alpha)}-\bar{S}e^{i(s-\alpha)}-\bar{M}e^{i(m-\alpha)}\} \quad (7)$$

where $\delta\nu_G=C_0G\cos(g-\alpha)=C_0Ge^{i(g-\alpha)}$, and $g$, $r$, $s$, and $m$ denote respectively the azimuths of vectors $\mathbf{G}$, $\bar{\mathbf{R}}$, $\bar{\mathbf{S}}$, and $\bar{\mathbf{M}}$. This equation indicates that the total Doppler shift is the real part of the sum of complex numbers expressed in exponential form. Vectorially speaking, there exists a vector $\mathbf{D}$ defined by

$$\bar{\mathbf{T}}=\bar{\mathbf{R}}+\bar{\mathbf{S}}+\bar{\mathbf{M}}$$

$$\mathbf{D}=\mathbf{G}-\bar{\mathbf{T}} \quad (8)$$

where $\bar{\mathbf{T}}$ represents the resultant vector of all effective velocities and is called the "total effective velocity." Equation (7) combined with equation (8) reveals that the vector $\mathbf{D}$ would cause the same amount of frequency shift as that caused by the ground velocity combined with the total effective velocities of various moving objects. Thus the total shift for a specific beam can be expressed by

$$\Delta\nu=C_0D\cos(d-\alpha)$$

or the real part of

$$\Delta\nu=C_0De^{i(d-\alpha)}, \quad (9)$$

where $d$ represents the azimuth of the vector $\mathbf{D}$. This vector is called the "effective Doppler velocity" and is expressed as a function of beam number and time.

## 3. FREQUENCY SHIFT OF A 4-BEAM DOPPLER SYSTEM

Since we are able to compute the Doppler frequency shift for each beam from the azimuth of the beam and the effective Doppler velocity, it is now feasible to obtain the frequency shift of a 4-beam Doppler system.

As shown schematically in figure 3, we assume that the beam nadir angle $\eta_0$ is kept constant for all beams regardless of the antenna rotation and that two vertical planes through the Doppler antenna include, respectively, a pair of opposite beams. The "Doppler heading" is defined as a horizontal vector dividing the angle between these planes into equal parts, $\psi_0$. This angle, which may be called the "beam horizontal angle," is constant, since antennas are rigidly attached to the vertically stabilized axis which is designed to rotate through a nulling process until the total frequency shifts between two opposite beams become identical. The final position thus reached is called in this paper the "null position" of antennas. The azimuth of the Doppler heading in this position is designated by $d_0$.

The azimuths of beams 1 through 4 identified in figure 3 are $\alpha_1=d_0+\psi_0$, $\alpha_2=d_0-\psi_0$, $\alpha_3=d_0+\psi_0+180$, and $\alpha_4=d_0-\psi_0+180$. These are put into equation (9) to obtain the total frequency shifts, which are the real parts of

$$\Delta\nu_1=C_0D_1e^{i(d_1-d_0-\psi_0)}=C_0e^{-id_0}D_1e^{i(d_1-\psi_0)},$$

$$\Delta\nu_2=C_0D_2e^{i(d_2-d_0+\psi_0)}=C_0e^{-id_0}D_2e^{i(d_2+\psi_0)},$$

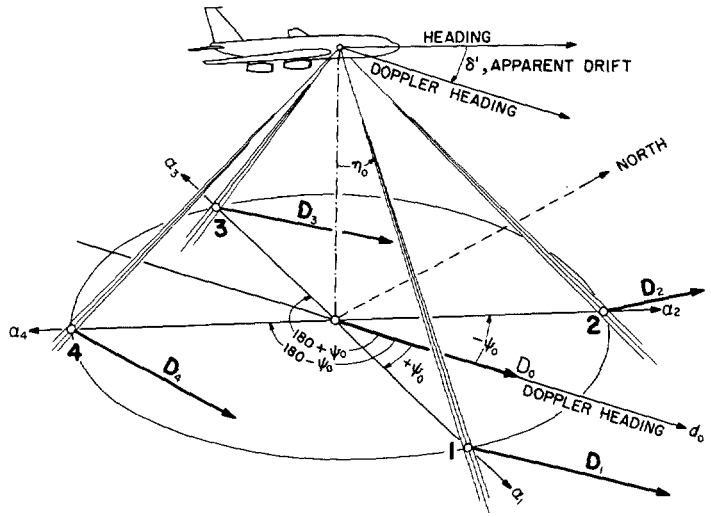


FIGURE 3.—Schematical diagram of a 4-beam Doppler system affected by effective Doppler velocities $\mathbf{D}_1$, $\mathbf{D}_2$, $\mathbf{D}_3$ and $\mathbf{D}_4$ defined as $\mathbf{D}=\bar{\mathbf{G}}-\bar{\mathbf{T}}$, where $\bar{\mathbf{T}}$ denotes the vector sum of the effective velocities of raindrops, spray, and surface water. Those beams under the influence of water in some form are called wet. When a beam is dry, it is affected only by the ground velocity. The Doppler heading in the figure is defined as a vector bisecting the forward beams.

$$\Delta\nu_3=-C_0D_3e^{i(d_3-d_0-\psi_0)}=-C_0e^{-id_0}D_3e^{i(d_3-\psi_0)},$$

and

$$\Delta\nu_4=-C_0D_4e^{i(d_4-d_0+\psi_0)}=-C_0e^{-id_0}D_4e^{i(d_4+\psi_0)}. \quad (10)$$

The condition for null position of antennas permits us to write

$$[\Delta\nu]_3^1=[\Delta\nu]_4^2 \quad \text{or} \quad \Delta\nu_1-\Delta\nu_3-\Delta\nu_2+\Delta\nu_4=0. \quad (11)$$

By using the frequency shifts for individual beams in equation (10), we express the null-position condition as

$$C_0e^{-id_0}\{D_1e^{i(d_1-\psi_0)}+D_3e^{i(d_3-\psi_0)}-D_2e^{i(d_2+\psi_0)}$$
$$-D_4e^{i(d_4+\psi_0)}\}=\text{imaginary number}. \quad (12)$$

Because of the fact that the real part of the left side of this equation must be zero to satisfy the null-position condition, the right side may be any imaginary number. Now we express the four terms within the bracket on the left side of the equation by a complex number, $Ye^{i\nu}$, and rearrange the terms to obtain

$$e^{-i\psi_0}(D_1e^{id_1}+D_3e^{id_3})=e^{i\psi_0}(D_2e^{id_2}+D_4e^{id_4})+Ye^{i\nu}. \quad (13)$$

Vectorially speaking, the sum of $\mathbf{D}_1+\mathbf{D}_3$ rotated by $\psi_0$ counterclockwise is identical to the sum of the vectors $\mathbf{D}_2+\mathbf{D}_4$ rotated by $\psi_0$ clockwise and $\mathbf{Y}$. These two rotated vectors are designated as $\overleftarrow{\mathbf{D}}_1+\overleftarrow{\mathbf{D}}_3$ and $\vec{\mathbf{D}}_2+\vec{\mathbf{D}}_4$, respectively.

Figure 4 shows schematically the graphical representation of the vectors given by equation (13). The origin of the polar coordinate is indicated by O, and the ends of the vectors $\overleftarrow{\mathbf{D}}_1+\overleftarrow{\mathbf{D}}_3$ and $\vec{\mathbf{D}}_2+\vec{\mathbf{D}}_4$, by A and B, respectively. The vector connecting B with A should be equal to $\mathbf{Y}$ by

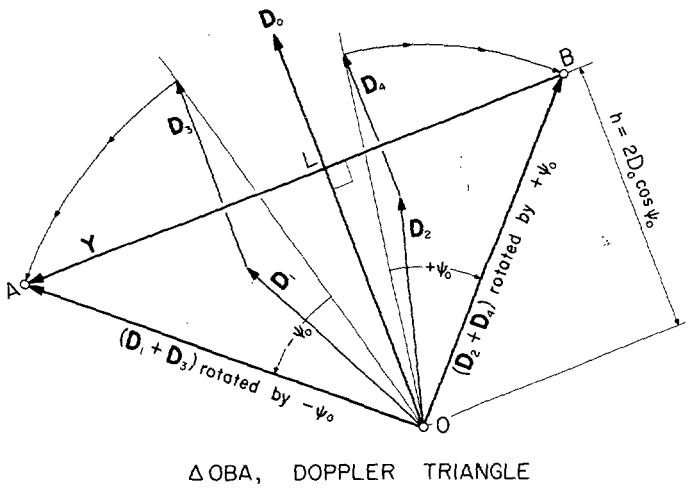


FIGURE 4.—A Doppler triangle consisting of two resultant vectors obtained by adding and rotating the effective Doppler velocities for opposite beams. A Doppler triangle determines the Doppler velocity, since the Doppler heading is perpendicular to its base and its altitude is proportional to the Doppler speed.

definition. Since the triangle OBA is frequently used in computing Doppler velocities over an area of non-uniform field of effective Doppler velocities, it may be identified as the "Doppler triangle."

## CHARACTERISTICS OF THE DOPPLER TRIANGLE

Once the Doppler triangle is determined, the Doppler heading and the Doppler ground speed can be obtained immediately. Equation (12) permits us to write

$$C_0 e^{-id_0} Y e^{iy} = \text{imaginary number},$$

which is reduced to

$$e^{-id_0} e^{iy} = i \text{ or } y - d_0 = \pm 90°. \tag{14}$$

That is to say, the Doppler heading is perpendicular to **Y** vector and points toward AB, the base of the triangle.

The Doppler speed can easily be obtained from the total frequency shift between the opposite beams in equation (10). Using the real parts for beams 1 and 3, we write the differential frequency shift as

$$[\Delta\nu]_3^1 = C_0\{D_1 \cos(d_1 - d_0 - \psi_0) + D_3 \cos(d_3 - d_0 - \psi_0)\}. \tag{15}$$

If we express the Doppler velocity measured at the null position by $\mathbf{D}_0$, the differential frequency shift should also be

$$[\Delta\nu]_3^1 = 2C_0 D_0 \cos\psi_0. \tag{16}$$

Thus we obtain

$$D_0 = \tfrac{1}{2} \sec\psi_0\{D_1 \cos(d_1 - \psi_0 - d_0) + D_3 \cos(d_3 - \psi_0 - d_0)\} \tag{17}$$

or

$$D_0 = \tfrac{1}{2} \sec\psi_0\{D_2 \cos(d_2 + \psi_0 - d_0) + D_4 \cos(d_4 + \psi_0 - d_0)\}. \tag{18}$$

The Doppler triangle reveals that the terms in the brackets in the right side of equations (17) and (18) are identical to the length OL=$h$, which is the altitude of the Doppler triangle in figure 4. The Doppler ground speed $D_0$, which is simply called the Doppler speed, can thus be expressed by

$$D_0 = \frac{h}{2} \sec\psi_0. \tag{19}$$

Equations (14) and (19) now permit us to obtain the Doppler speed and the Doppler heading when the antennas are in null position. The effective Doppler velocities **D** causing frequency shifts which are measured by four beams may not necessarily be uniform for the application of this result.

## FLIGHT OVER A UNIFORM D FIELD

If a flight is made over an area of a uniform effective Doppler velocity **D** defined by equation (8), the Doppler triangle is isosceles and the Doppler velocity can be expressed simply by

$$\mathbf{D}_0 = \mathbf{D} = \mathbf{G} - \overline{\mathbf{T}}. \tag{20}$$

It is evident that the measured Doppler velocity is the vector difference between the ground velocity of the aircraft and the resultant velocity of all effective velocities of raindrops, spray, and the water surface. Since the vector $\overline{\mathbf{T}}$ is caused mostly by the return signal from the moving water in some form, a beam is identified as a "wet beam" when it receives the signal affected by $\overline{\mathbf{T}}$. In the special case in which the same $\overline{\mathbf{T}}$ is applicable to two or more beams, they are called "uniformly wet beams."

## UNIFORMLY WET ADJACENT BEAMS

When two adjacent beams pointing forward are uniformly wet and others are dry, the **D** field can be expressed by

$$\mathbf{D}_1 = \mathbf{D}_2 = \mathbf{G} - \overline{\mathbf{T}} \qquad \text{and} \qquad \mathbf{D}_3 = \mathbf{D}_4 = \mathbf{G}.$$

The Doppler triangle is undoubtedly isosceles, thus permitting us to write

$$\mathbf{D}_0 = \mathbf{G} - \tfrac{1}{2}\overline{\mathbf{T}}. \tag{21}$$

This relationship is also applicable to all cases when the adjacent beams are uniformly wet, and it can be stated that the Doppler velocity is the ground velocity of the aircraft less one-half of the effective ground velocities.

## SINGLE WET BEAM

It is rather unlikely that adjacent beams are uniformly wet while the plane is flying in or near a precipitating cloud. There will be many cases when only one beam is wet while others are completely dry. In such cases, the Doppler triangle is no longer isosceles, and a more complicated vector diagram as shown in figure 5 should be solved.

First we assume that all beams are dry and establish a Doppler triangle A'OB, the two sides of which are $2G$ by

795-456 O - 66 - 4

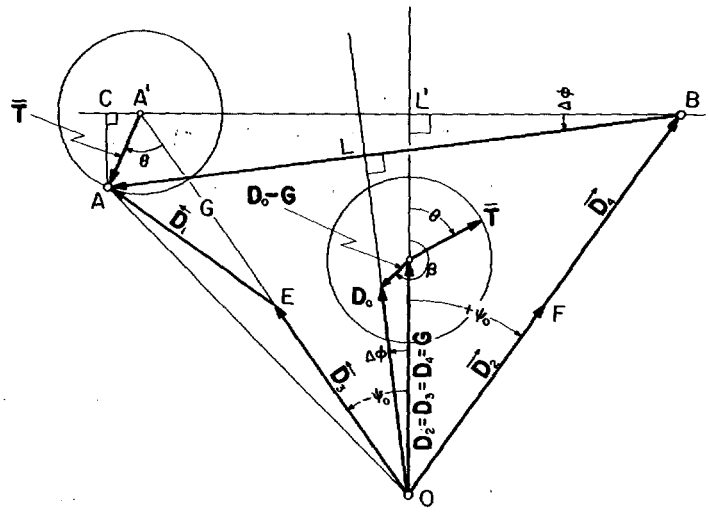


FIGURE 5.—Construction of a Doppler triangle to solve Doppler velocities of a 4-beam system when one of the beams is wet. The result reveals that the vector difference $\mathbf{D}_0-\mathbf{G}$ is always in the direction $90-\psi_0$ or $270-\psi_0$ from the ground velocity and that moving objects, regardless of their total velocities, do not influence the measured Doppler velocity if their direction of motion is $90+\psi_0$ or $270+\psi_0$ from the ground velocity.

definition. Then we consider that beam $l$ becomes wet, influenced by the total effective velocity $\overline{\mathbf{T}}$ in an angle $\theta$ from the direction of the ground velocity. Thus we write

$$\mathbf{D}_1=\mathbf{G}-\overline{\mathbf{T}} \qquad \text{and} \qquad \mathbf{D}_2=\mathbf{D}_3=\mathbf{D}_4=\mathbf{G}.$$

The Doppler triangle now deforms into AOB, resulting in a deviation of the Doppler velocity from the ground velocity **G**.

The angle between the vectors $\mathbf{D}_0$ and **G** expressed by $\Delta\phi$ is always equal to $\angle ABA'$, thus permitting us to write the length of the line BC as

$$\overline{T}\cos(\theta-\psi_0)\cot\Delta\phi=4G\sin\psi_0+\overline{T}\sin(\theta-\psi_0), \quad (22)$$

which can be reduced to

$$\Delta\phi=g-d_0\cong\frac{\overline{T}\cos(\theta-\psi_0)}{4G\sin\psi_0} \quad (23)$$

when $\overline{T}$ is very small compared with the ground speed. This assumption is justifiable in most cases unless a beam attenuates appreciably inside fast-moving precipitation.

The altitude of the Doppler triangle is now obtained as

$$h=2G\cos(\Delta\phi+\psi_0), \quad (24)$$

which can be reduced to

$$h=2G(\cos\psi_0-\Delta\phi\sin\psi_0), \quad (25)$$

since $\Delta\phi$ is already assumed to be small. From equations (19) and (23) we finally obtain the Doppler speed,

$$D_0=G(1-\Delta\phi\tan\psi_0)=G-\tfrac{1}{4}\overline{T}\cos(\theta-\psi_0)\sec\psi_0. \quad (26)$$

In order to determine $\beta$, the direction of the vector $\mathbf{D}_0-\mathbf{G}$ measured from the ground velocity of the aircraft, we use equations (23) and (26) and write

$$\cot\beta=\frac{G-D_0\cos\Delta\phi}{D_0\sin\Delta\phi}\cong\frac{D_0+\frac{1}{4}\overline{T}\cos(\theta-\psi_0)\sec\psi_0-D_0\cos\Delta\phi}{D_0\Delta\phi}$$

When $\overline{T}$ is small compared with $G$, the equation can be reduced to

$$\cot\beta\cong\frac{1}{2}\Delta\phi+\frac{G}{D_0}\tan\psi_0\cong\tan\psi_0. \quad (27)$$

In fact, equation (26) gives the maximum and minimum values of $D_0$ as $G+\frac{1}{4}\overline{T}$ and $G-\frac{1}{4}\overline{T}$, respectively. The Doppler speed divided by the ground speed thus varies within a very small range,

$$1-\frac{\overline{T}}{4G}<\frac{D_0}{G}<1+\frac{\overline{T}}{4G}.$$

On the other hand, $\Delta\phi$ is usually small compared with $\psi_0$.

Equation (27) thus reveals an important result that $\beta=90-\psi_0$ or $\beta=270-\psi_0$. That is to say, the vector difference $\mathbf{D}_0-\mathbf{G}$ is always oriented in a fixed direction with respect to the ground velocity of the aircraft. According to equation (26), the absolute value of this difference reaches zero when $\theta=\psi_0\pm90$, and $\frac{1}{4}\overline{T}$, when $\theta=\psi_0$ or $\theta=\psi_0+180$. These results indicate that one wet beam does not alter the Doppler velocity at all if the azimuth of the beam is perpendicular to the total effective velocity and also that the maximum influence, $\frac{1}{4}\overline{T}$, appears when the wet beam is in the direction of the total effective velocity.

### UNIFORMLY WET OPPOSITE BEAMS

The equations for computing Doppler shift, involving opposite beams which are uniformly wet, can be obtained in a manner similar to that applied to a single wet beam. The Doppler triangle in this case should be constructed simply by changing $\overline{T}$ into $2\overline{T}$. The final equations thus obtained are

$$g-d_0=\Delta\phi=\frac{\overline{T}\cos(\theta-\psi_0)}{2G\sin\psi_0} \quad (28)$$

and

$$D_0=G-\tfrac{1}{2}\overline{T}\cos(\theta-\psi_0)\sec\psi_0. \quad (29)$$

### FOUR DRY BEAMS

When an aircraft flies horizontally over the ground keeping all beams dry, the problem becomes extremely simple, permitting us to draw a group of isodops, each of which represents a line of a constant Doppler shift.

By applying equation (4) to the ground velocity **G**, the partial frequency shift is expressed by

$$\delta\nu_G=\frac{2\nu_0}{c}G\cos\gamma_G, \quad (30)$$

where $\gamma_G$ denotes the beam inclination with respect to **G**.

Now we choose the $x$ axis in the direction of G through the aircraft subpoint, $y$ axis in the 90° direction from the $x$ axis, and $z$ axis upward. The equation of the cone representing the frequency shift $\delta\nu_G$,

$$y^2+(z-H)^2=x^2\tan^2\gamma_G,$$

and the equation of the ground,

$$z=0,$$

are combined with equation (30) to eliminate $z$ and $\gamma_G$. Thus we obtain

$$\left(1-\frac{4G^2\nu_0^2}{c^2\delta\nu_G^2}\right)x^2-y^2=H^2, \tag{31}$$

where $H$ is the height of the aircraft above the ground. This equation indicates that a group of isodops consisting of hyperbolas moves with an aircraft. The line of zero shift expressed by $x=0$ is a straight line perpendicular to the ground velocity of the aircraft translated to the subaircraft point.

In order to avoid a broadening of the power spectrum of the return frequency, each antenna is designed to illuminate a narrow area along an isodop. Especially when an aircraft flies over water, the change in backscattering cross section as obtained by Wiltse, Schlesinger, and Johnson [10] and Grant and Yaplee [5] reduces the maximum return frequency, thus resulting in a computed ground speed lower than it should be.

## 4. INFLUENCE OF VERTICAL VELOCITIES

The frequency shift by a single Doppler beam is affected by the vertical motions of both aircraft and the raindrops. Equation (1), excluding the horizontal speed, is now written as

$$\delta\nu'=-\frac{2\nu_0}{c}(G'+\bar{R}')\cos\eta_0, \tag{32}$$

where $\delta\nu'$ denotes the contribution of the vertical motions to the frequency shift; $G'$, the vertical speed of the aircraft; and $\bar{R}'$, the effective fall speed of the raindrops.

If we assume that there is no horizontal motion of the raindrops, as in the case of stationary showers, the total frequency shift for a single beam with its beam nadir angle $\eta_0$ and azimuth $\alpha$ can be written as

$$\begin{aligned}\Delta\nu'&=\delta\nu_G+\delta\nu_G'+\delta\nu_R'\\&=C_0G\cos(g-\alpha)-C_0(G'+\bar{R}')\cot\eta_0,\end{aligned} \tag{33}$$

where $g$ denotes the azimuth of the ground velocity.

Next we express the direction of G measured from the Doppler velocity by $\Delta\phi$ and write the azimuths of each beam as: $\alpha_1=g-\Delta\phi+\psi_0$, $\alpha_2=g-\Delta\phi-\psi_0$, $\alpha_3=g-\Delta\phi+\psi_0-180$, and $\alpha_4=g-\Delta\phi-\psi_0+180$. Putting these azimuths into equation (33), we obtain the frequency shift for each beam. Namely,

$$\begin{aligned}\Delta\nu_1'&=C_0G\cos(\Delta\phi-\psi_0)-C_0(G'+\bar{R}_1')\cot\eta_0,\\\Delta\nu_2'&=C_0G\cos(\Delta\phi+\psi_0)-C_0(G'+\bar{R}_2')\cot\eta_0,\\\Delta\nu_3'&=-C_0G\cos(\Delta\phi-\psi_0)-C_0(G'+\bar{R}_3')\cot\eta_0,\\\Delta\nu_4'&=-C_0G\cos(\Delta\phi+\psi_0)-C_0(G'+\bar{R}_4')\cot\eta_0.\end{aligned} \tag{34}$$

The differential frequency shifts, defined as the difference between the frequency shifts measured by a pair of opposite beams, are expressed by

$$[\Delta\nu]_3^1=2C_0G\cos(\Delta\phi-\psi_0)-C_0(\bar{R}_1'-\bar{R}_3')\cot\eta_0$$

and

$$[\Delta\nu]_4^2=2C_0G\cos(\Delta\phi+\psi_0)-C_0(\bar{R}_2'-\bar{R}_4')\cot\eta_0. \tag{35}$$

It should be noted that the vertical velocity G′ does not alter the differential frequency shift.

When the null position of the beams is reached, the differential frequency shifts expressed by equation (35) must be equal. Thus we have

$$4G\sin\Delta\phi\sin\psi_0=(\bar{R}_1'-\bar{R}_2'-\bar{R}_3'+\bar{R}_4')\cot\eta_0.$$

The angle $\Delta\phi=g-d_0$ can now be computed from

$$\Delta\phi\cong\sin\Delta\phi=\frac{\cot\eta_0}{4G\sin\psi_0}(\bar{R}_1'-\bar{R}_2'-\bar{R}_3'+\bar{R}_4'). \tag{36}$$

This result reveals that the direction of measured Doppler velocity $\mathbf{D}_0$ differs slightly from that of the ground velocity G unless the beams are all dry or

$$\bar{R}_1'-\bar{R}_2'-\bar{R}_3'+\bar{R}_4'=0. \tag{37}$$

Finally, the differential shifts from equations (16) and (35) are equated to obtain

$$\begin{aligned}2D_0\cos\psi_0&=2G\cos(\Delta\phi-\psi_0)-(\bar{R}_1'-\bar{R}_3')\cot\eta_0\\2D_0\cos\psi_0&=2G\cos(\Delta\phi+\psi_0)-(\bar{R}_2'-\bar{R}_4')\cot\eta_0\end{aligned}$$

which can be reduced, for small values of $\Delta\phi$, to

$$D_0=G-\tfrac{1}{4}(\bar{R}_1'+\bar{R}_2'-\bar{R}_3'-\bar{R}_4')\cot\eta_0\sec\psi_0. \tag{38}$$

It is obvious that the Doppler speed differs from the ground speed unless

$$\bar{R}_1'+\bar{R}_2'-\bar{R}_3'-\bar{R}_4'=0. \tag{39}$$

The Doppler velocity is identical to the ground velocity only when equations (37) and (39) are simultaneously satisfied. That is to say, the opposite beams must be uniformly wet ($\bar{R}_1'=\bar{R}_3'$ and $\bar{R}_2'=\bar{R}_4'$). This certainly includes the case when all beams are uniformly wet.

## 5. ERRORS IN WIND MEASUREMENTS RESULTING FROM WET BEAMS

For the purpose of developing equations for Doppler wind computation, a so-called "navigation triangle" is frequently used. The three sides of the triangle consist of

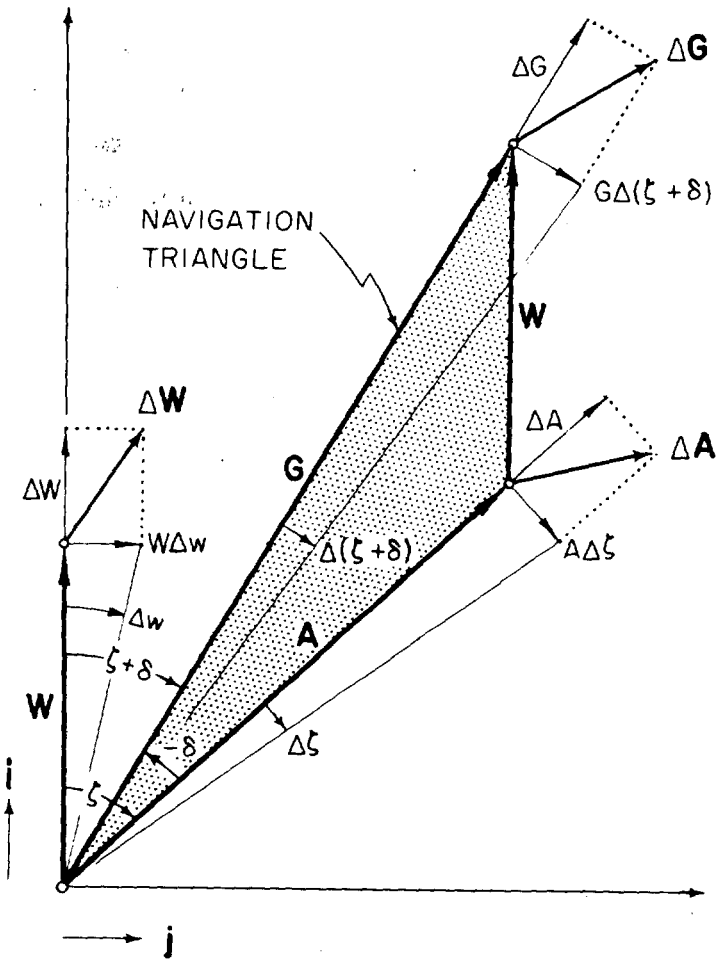


FIGURE 6.—The navigation triangle and the vector errors in the true air velocity (**A**), the ground velocity (**G**), and the wind velocity (**W**). The errors are also expressed by their components in the radial and tangential directions. $\delta$ denotes the drift angle; $\zeta$, the crosswind angle of the aircraft heading; and $\alpha$, the azimuth of the wind velocity.

the true air speed vector **A** (true air velocity), the wind velocity **W**, and the ground speed vector of aircraft **G** (ground velocity). These three vectors are always closed as shown in figure 6, and are bound together by a vector equation

$$\mathbf{W}=\mathbf{G}-\mathbf{A}. \tag{40}$$

If all four beams are dry, a Doppler system measures the ground velocity **G**. When one or more beams is wet, however, a Doppler system computes an erratic wind by solving an erratic navigation triangle, thus

TABLE 1.—*Estimate of the terms contributing to the errors in Doppler winds*

| Terms | Symbols | Coefficient | Speed | Effective Speed |
|---|---|---|---|---|
| Ground speed of aircraft | $G$ | 1.0 | 100 to 600 kt. | 0 to 300 m./sec. |
| Vertical speed of aircraft | $G'$ | 1.0 | 0 to ± 100 ft./sec. | 0 to 30 m./sec. |
| Falling speed of raindrops | $R'$ | 0–1.0 | 0 to 30 ft./sec. | 0 to 20 m./sec. |
| Horizontal speed of raindrops | $R$ | 0–1.0 | 0 to ± 60 kt. | 0 to 30 m./sec. |
| Horizontal speed of spray | $S$ | 0–0.3 | 0 to 100 kt. | 0 to 15 m./sec. |
| Horizontal speed of water surface | $M$ | 0–1.0 | 0 to ± 10 kt. | 0 to 10 m./sec. |

TABLE 2.—*Maximum error in Doppler winds obtained under various conditions of four beams. The total effective velocity* $\overline{\mathbf{T}}$, *as defined by equation (8), is the sum of the effective velocities of raindrops, spray, and water surface. The effective fall velocity of raindrops* $\overline{\mathbf{R}}'$ *is defined as* $k_R\overline{\mathbf{R}}'$, *which is identical to the fall velocity when a beam locks onto a heavy precipitation.*

| Conditions of beams | Maximum error due to $\overline{T}$ | Maximum error due to $\overline{R}'$ |
|---|---|---|
| Four dry beams | zero | zero |
| Single wet beam | $\frac{1}{4}\overline{T}\sec\psi_0$ | $\frac{1}{4}\overline{T}\cot\eta_0\sec\psi_0$ |
| Uniformly wet adjacent beams. | $\frac{1}{2}\overline{T}$ | $\frac{1}{2}\overline{T}\cot\eta_0\sec\psi_0$ |
| Uniformly wet opposite beams. | $\frac{1}{2}\overline{T}\sec\psi_0$ | zero |
| Four uniformly wet beams. | $\overline{T}$ | zero |
| Four wet beams | $\frac{1}{2}(\overline{T}_1+\overline{T}_2+\overline{T}_3+\overline{T}_4)$ | $\frac{1}{4}(\overline{R}'_1+\overline{R}'_2+\overline{R}'_3+\overline{R}'_4)\cot\eta_0\sec\psi_0$ |

$$\mathbf{W}+\Delta\mathbf{W}_*=\mathbf{D}_0-\mathbf{A}, \tag{41}$$

where $\Delta\mathbf{W}_*$ denotes the wind velocity error. By using equation (40), the wind velocity error is now written as

$$\Delta\mathbf{W}_*=\mathbf{D}_0-\mathbf{G}, \tag{42}$$

which indicates that the vector difference between the measured Doppler velocity and the ground velocity of the aircraft represents the wind velocity error, even though there exists no error in the computation of Doppler velocity.

With the use of the equations obtained so far, an estimate of errors due to wet beams is now attempted. As a basis of quantitative evaluation, estimated values of the effective speeds are given in table 1. The ground speed may vary within a wide range of probably 100 to 600 kt., depending upon the aircraft type and tailwind conditions. The vertical velocity of the aircraft has nothing to do with the Doppler velocity when measured with a 4-beam system. The terms involving raindrops, spray, and moving water surface could vary considerably from place to place. Their values in the table are based upon a crude estimate and are subject to revision when more data become available in the future.

From the practical point of view, it is necessary to know the maximum errors in wind velocities measured under various conditions of the Doppler beams. Table 2 summarizes such maximum errors, or the maximum differences between $\mathbf{D}_0$ and **G** vectors. There should, of course, be no error when four beams are dry. The falling velocity of raindrops is free from the wind velocity error provided the opposite beams are uniformly wet, while the horizontal effective velocity always induces a possible maximum error in wind velocity even if one or more beams is uniformly wet.

## 6. ERRORS IN WIND MEASUREMENT WITH DRY BEAMS

It has been revealed in the previous sections that the Doppler winds measured under wet-beam conditions differ from true winds. The errors can be computed theoretically if we assume that measured Doppler veloc-

ities are correct and that the effective velocities are known.

In the actual measurements, it is necessary to assume that there are errors in the true air speed computed from differential pressure and air temperature, as well as in the ground velocity determined by the Doppler system. Since these errors are usually very small, we differentiate equation (40) and form a scalar product of a unit vector **i** pointing toward the true wind vector. Thus we have

$$\mathbf{i}\cdot d\mathbf{W}=\mathbf{i}\cdot d\mathbf{G}-\mathbf{i}\cdot d\mathbf{A},$$

which, after changing $d$ into $\Delta$, can be expanded into

$$\Delta W=\Delta G\cos(\zeta+\delta)-\Delta(\zeta+\delta)G\sin(\zeta+\delta)-\Delta A\cos\zeta+\Delta\zeta A\sin\zeta$$
$$=\Delta G\cos(\zeta+\delta)-G\Delta\delta\sin(\zeta+\delta)-\Delta A\cos\zeta \quad (43)$$

where $\Delta G$ denotes the ground-speed error; $\Delta A$, the true air-speed error; $\Delta\delta$, the drift-angle error; and $\zeta$, the crosswind angle, the direction of aircraft heading measured clockwise from the true wind direction (see fig. 6).

In a similar manner we obtain a scalar product of another unit vector **j** pointing 90° from the true wind vector, thus

$$\mathbf{j}\cdot d\mathbf{W}=\mathbf{j}\cdot d\mathbf{G}-\mathbf{j}\cdot d\mathbf{A},$$

which is expanded into

$$W\Delta w=\Delta G\sin(\zeta+\delta)+\Delta(\zeta+\delta)G\cos(\zeta+\delta)-\Delta A\sin\zeta-\Delta\zeta A\cos\zeta$$
$$=\Delta G\sin(\zeta+\delta)+G\Delta\delta\cos(\zeta+\delta)-\Delta A\sin\zeta+\Delta\zeta W, \quad (44)$$

where $\Delta w$ represents the error in wind direction. Dividing both sides by $W$, we obtain

$$\Delta w=\frac{\Delta G}{W}\sin(\zeta+\delta)+\frac{G\Delta\delta}{W}\cos(\zeta+\delta)-\frac{\Delta A}{W}\sin\zeta+\Delta\zeta. \quad (45)$$

It should be noted that the error in aircraft heading, which is equal to that of the crosswind angle $\Delta\zeta$, contributes to the wind direction error in exactly the same amount. That is to say, a 1° error in the aircraft heading rotates the wind direction by 1°. Its consequence is extremely small.

The drift-angle error $\Delta\delta$ is important, since, as indicated by equation (45), it is multiplied by the factor of $G/W$ which is a large quantity for low wind speed and fast-moving aircraft. Equation (43) reveals that the effect of the drift angle upon the wind-speed error is also appreciable.

When the wind speed is relatively low compared with the true air speed of an aircraft, we may assume that $\delta$ is much smaller than $\zeta$. This assumption permits us to reduce equations (43) and (45) to

$$\Delta W=(\Delta G-\Delta A)\cos\zeta-G\Delta\delta\sin\zeta \quad (46)$$

and

$$\Delta w=\frac{(\Delta G-\Delta A)}{W}\sin\zeta+\frac{G\Delta\delta}{W}\cos\zeta, \quad (47)$$

in which $G$ may be assumed to be constant since $W$ is small. The term $\Delta\zeta$ has been eliminated because of its insignificant influence. These equations indicate that the errors in ground speed measured by a Doppler system and the true air speed contribute to the wind error in the form of a difference, $\Delta G-\Delta A$, thus suggesting the possibility of applying corrections as one quantity. In fact, the Research Flight Facility [8] has been correcting the true air speed in an attempt to reduce this difference to zero. Their results are known to be very good.

We now express this difference by $\Delta E$ and write equations (46) and (47) in trigonometric form

$$\Delta W=\Delta E\cos\zeta-G\Delta\delta\sin\zeta\equiv\Delta a_1\sin(\zeta+\theta_1) \quad (48)$$

$$W\Delta w=\Delta E\sin\zeta+G\Delta\delta\cos\zeta\equiv\Delta a_2\sin(\zeta+\theta_2), \quad (49)$$

where $\Delta a_1$, $\Delta a_2$, $\theta_1$, and $\theta_2$ are constants. By putting $\zeta=0°$ and $\zeta=90°$ into the above equations, we have

$$\Delta E=\Delta a_1\sin\theta_1 \text{ and } -G\Delta\delta=\Delta a_1\cos\theta_1,$$
$$\Delta E=\Delta a_2\cos\theta_2 \text{ and } G\Delta\delta=\Delta a_2\sin\theta_2. \quad (50)$$

The constants $\Delta a_1$ and $\Delta a_2$ are obviously the amplitudes of sinusoidal curves representing measured wind speed $W+\Delta W$ and measured wind direction times the true wind speed, $W\Delta w$, respectively.

It is evident, from equation (50), that the amplitudes of the sinusoidal curves of $W+\Delta W$ and $W\Delta w$ as functions of $\zeta$ are identical, thus

$$\Delta a=\Delta a_1=\Delta a_2=(\Delta E^2+G^2\Delta\delta^2)^{1/2}. \quad (51)$$

Equation (50) also reveals that the phase angles $\theta_1$ and $\theta_2$ are not independent but are related by

$$\theta_2=\theta_1-90°. \quad (52)$$

We shall now express $\Delta E$ and $\Delta\delta$ as functions of $\Delta a$ and $\theta_1$ so that these errors can be computed by measuring the amplitude $\Delta a$ and the phase angle $\theta_1$ from the actual winds measured by the Doppler wind system. For this purpose, equations (50), (51), and (52) are combined into

$$\Delta E=\Delta a\sin\theta_1 \text{ and } \Delta\delta=-\frac{\Delta a}{G}\cos\theta_1. \quad (53)$$

The determination of these errors thus requires continuous changes in the aircraft heading until the wind speed and direction expressed as a function of the crosswind angle $\zeta$ clearly indicate definite sinusoidal variations. For the accurate determination of both amplitude and phase angle, however, it is often necessary to complete a loop flight during which the crosswind angle changes by 360°.

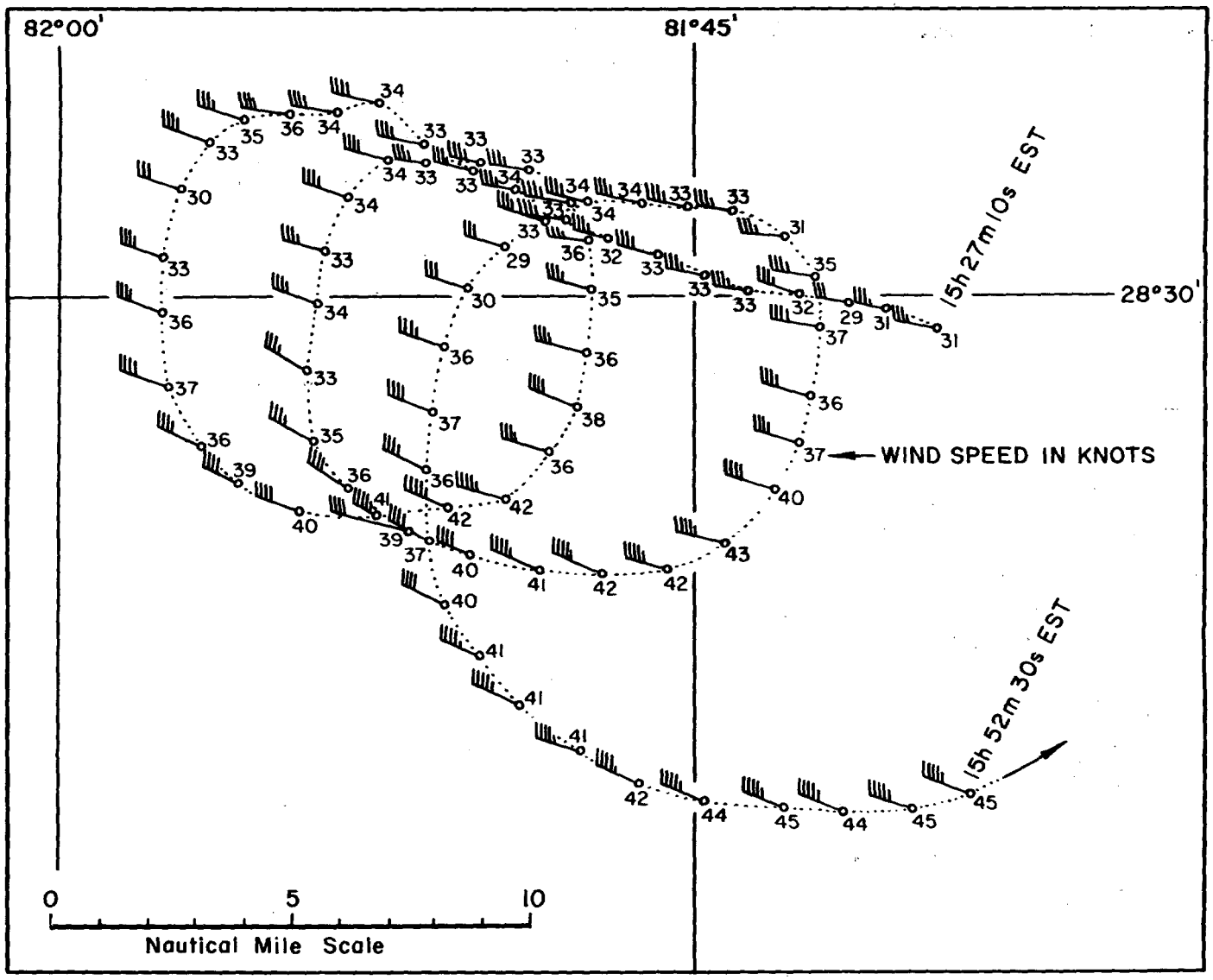


FIGURE 7.—The Doppler winds along three loops flown over central Florida on November 6, 1963 at 11,000-ft. altitude. The area was in the cold sector of a weak cyclone and free from clouds.

## 7. TEST FLIGHT FOR DOPPLER-WIND CALIBRATION

For the purpose of calibrating Doppler winds measured under a dry-beam condition, a loop flight pattern was designed by the author and flown by one of the DC–6B's of the Research Flight Facility. Central Florida and Oklahoma were selected as the flight areas because of abundant lakes and highways which can easily be identified in pictures taken from about a 10,000-ft. altitude. Figure 7 shows the uncorrected Doppler winds plotted along three loops flown by the DC–6B at an altitude of about 11,000 ft. over central Florida on November 6, 1963. The small numbers entered next to the wind symbols denote the wind speed.

A first glance at the wind field in the figure gives the impression that Doppler winds include few or no errors. A detailed examination of both speed and direction, however, reveals a tendency for the speed to increase as the aircraft changes its heading from south to southeast, then to the east. This evidence raises a suspicion of some errors.

Equations (46) and (47), as well as equations (50) and (51), indicate that the wind direction and speed fluctuate as sinusoidal curves if they are computed from quantities that include small errors. Such a fluctuation permits us to detect very small errors in both drift angle and true air speed and Doppler speed combined.

Figure 8 was prepared in an attempt to evaluate the errors from the characteristic fluctuation in both wind direction and speed. The wind data used in plotting figure 7 were again used for the purpose of revealing the

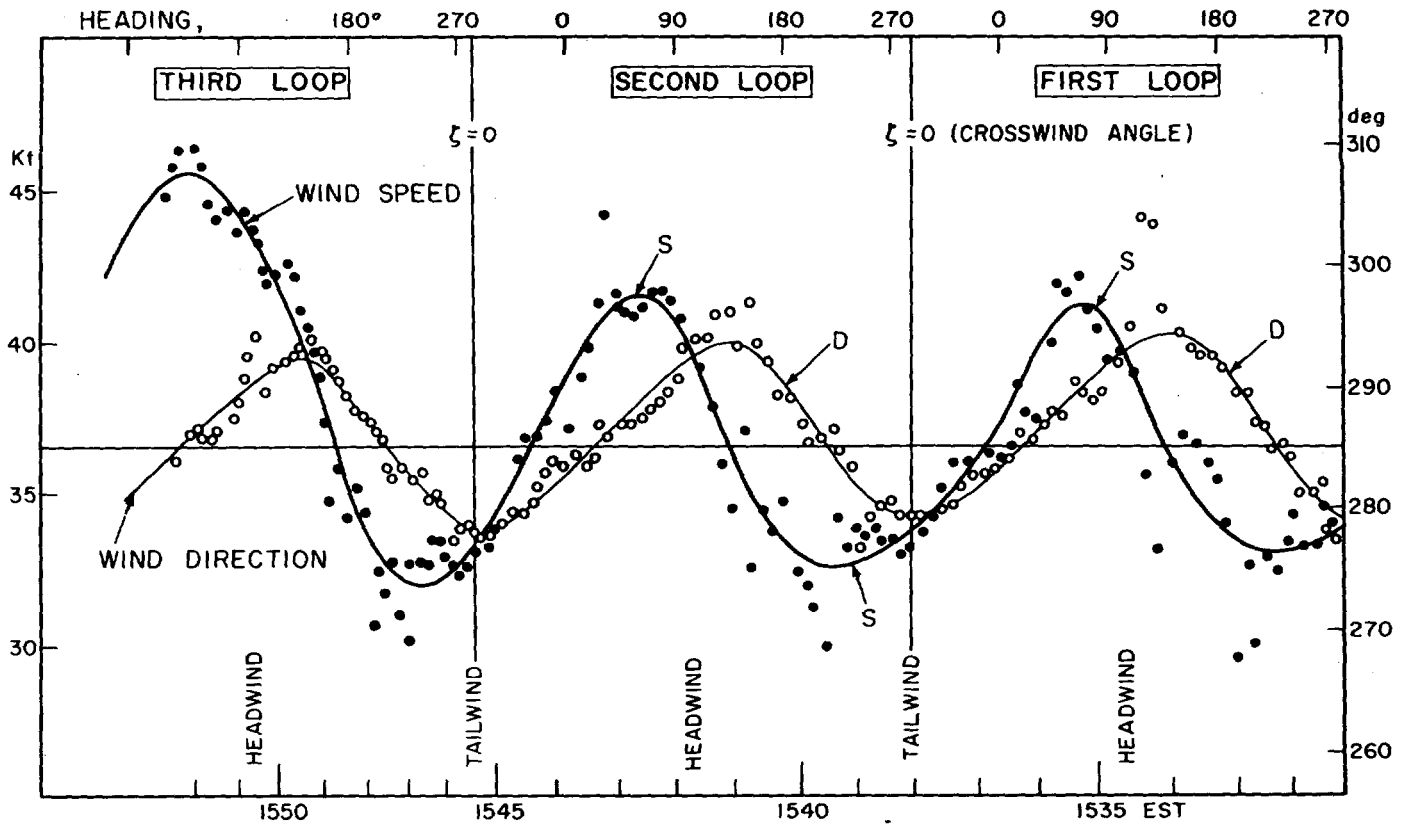


FIGURE 8.—Further evaluation of the Doppler winds presented in the previous figure. In this case, the wind speed and the direction are plotted against the aircraft heading for the purpose of determining the amplitudes and the phase angles of the fluctuation caused by small remaining errors. Estimated true air speed error and drift angle error are 1.9 kt. and −0.87°, respectively.

existence of errors through a different method of presentation. The amplitude of the fluctuation and the phase angle are thus measured out of these curves and presented in table 3. The errors $\Delta E$ and $\Delta\delta$ were then computed from equations (52) and (53). The errors, averaged for three loops, reveal the necessity of subtracting 1.9 kt. from the true air speed and adding 0.87° to the drift angle obtained by the Doppler system. It should be noted that the correction of such small quantities is necessary to eliminate fictitious winds which are not usable in computing mesoscale wind fields.

For the purpose of presenting the fluctuation of both wind speed and direction resulting from the percent error in the ground speed, $\Delta G/G$, and in the true air speed, $\Delta A/A$, figures 9 and 10 were obtained by using the computer output programed for the conditions of the Florida test flight case expressed by

| | |
|---|---|
| Mean wind speed | 36. 5 kt. |
| Mean wind direction | 286° |
| Mean true air speed | 221 kt. |

The wind direction and speed were computed at 1-percent intervals of error, positive for the ground speed and negative for the true air speed, to allow direct comparison of the fluctuation. As expected, the fluctuations of fictitious winds due to $\Delta G$ and $\Delta A$ are similar to each other, especially when the percent error is small. This is why the error in the ground speed can be corrected by changing the true air speed. The fluctuation of measured wind due only to the drift angle error is also shown in figure 11. The computer inputs are the same as for the previous ones, except for the intervals, 1° of the drift-angle error.

TABLE 3.—*The amplitude ($\Delta a$) and phase angle ($\theta_1$) of wind speed and direction plotted against the crosswind angle. The error, $\Delta E=\Delta G-\Delta A$, and the drift-angle error, $\Delta\delta$, are computed from $\Delta a$ and $\theta_1$ using equations (52) and (53). The diameters of the three loops are 9, 8, and 12 n. mi., respectively. The speed and direction fluctuations for the third loop seem to include the variation in the wind itself.*

| | | First Loop | Second Loop | Third Loop | Mean of 3 Loops |
|---|---|---|---|---|---|
| ($\Delta a$) | from speed | 4.1 kt. | 4.3 kt. | 6.7 kt. | 5.0 kt. |
| | from direction | 2.9 kt. (7.5°) | 2.9 kt. (7.5°) | 2.7 kt. (7.1°) | 2.8 kt. |
| | mean value | 3.5 kt. | 3.6 kt. | 4.7 kt. | 3.9 kt. |
| ($\theta_1$) | from speed | 30° | 30° | 40° | 33° |
| | from direction | 20° | 20° | 30° | 23° |
| | mean value | 25° | 25° | 35° | 28° |
| ($\Delta E$) | from speed | 2.0 kt. | 2.1 kt. | 4.3 kt. | 2.8 kt. |
| | from direction | 1.0 kt. | 1.0 kt. | 1.4 kt. | 1.1 kt. |
| | mean value | 1.5 kt. | 1.5 kt. | 2.8 kt. | 1.9 kt. |
| ($\Delta\delta$) | from speed | −0.94° | −0.96° | −1.35° | −1.08° |
| | from direction | −0.70° | −0.70° | −0.60° | −0.66° |
| | mean value | −0.82° | −0.83° | −0.97° | −0.87° |

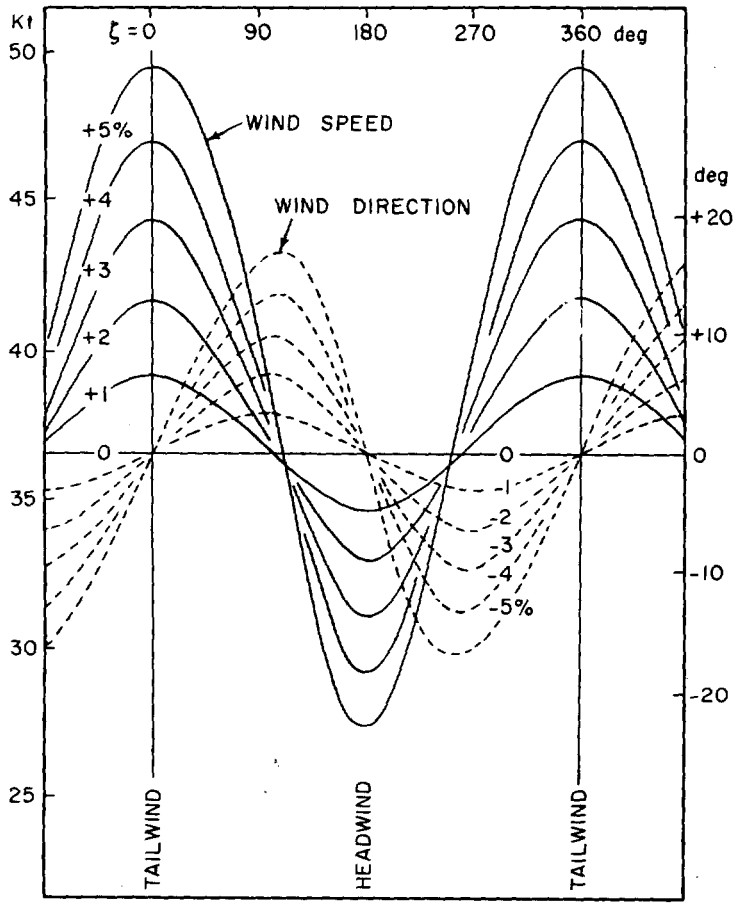


FIGURE 9.—Fluctuation of measured Doppler winds corresponding to the error in the ground speed expressed by the percent of $\Delta G/G$. Note that the fluctuation of the wind direction lags 90° behind the wind speed.

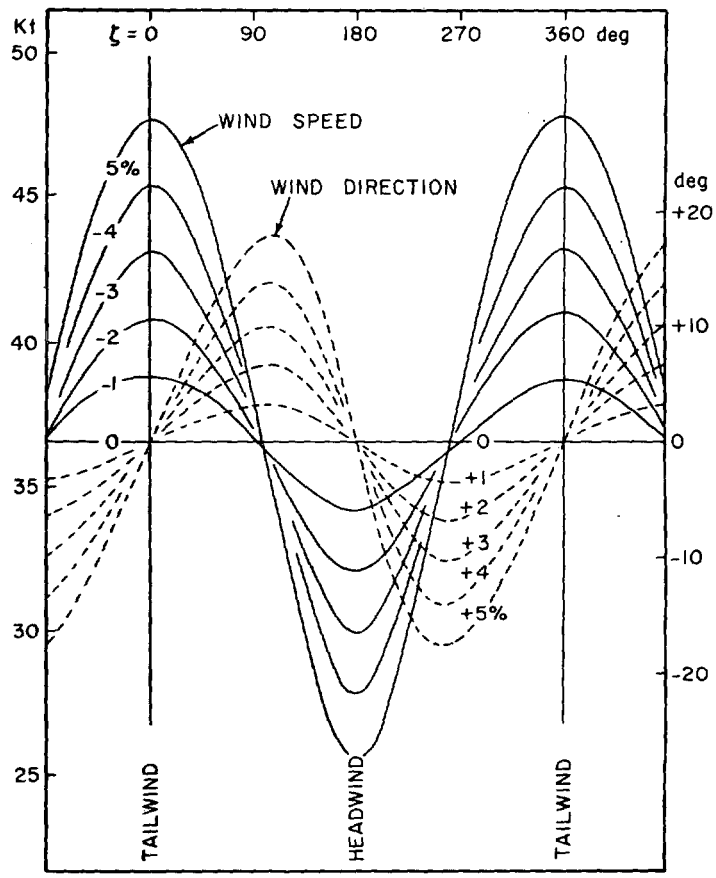


FIGURE 10.—Fluctuation of measured Doppler winds corresponding to the error in the true air speed given in the percent of $\Delta A/A$. When the percent is small, the wind speed variation as well as the direction variation is almost identical to that of the previous figure. This is why the ground speed error can be corrected by changing the true air speed.

It should be noted that there is a 90°-phase shift between the wind speed and the direction curves. This characteristic has already been clarified by equations (50) and (51) which indicate that an identical phase shift should exist even when errors in true air speed, ground speed, and and Doppler heading come into effect simultaneously.

## 8. PHOTOGRAMMETRIC EVALUATION OF DC-6B DOPPLER WINDS

When the flight test discussed in the previous section was made over Florida, two 35-mm., double-frame size cameras were mounted on opposite windows of the DC-6B. Both cameras, equipped with 21-mm. wide-angle lenses, were exposed simultaneously by the pulses supplied by the plane's digital system at 20-sec. intervals, thus obtaining a perfect synchronization between the exposure and the digital times.

An example of a pair of the photographs taken simultaneously through right and left windows appears in figure 12. The photographs include isolines of nadir and horizontal angles at 10° intervals. By using transfer height grids similar to those developed by Fujita [3], significant landmarks in each pair of right and left photographs were transferred to a chart in the scale of a topographic map covering the test-flight area. After the transfer had been completed, the chart was placed on the map in such a position and orientation that all available landmarks on the chart and the map showed the best possible agreement. Figure 13 represents the photographic areas with landmarks and the topographic map. It was found that the sub-aircraft points thus determined are accurate to about 0.1 mi.

The positions of the aircraft at 20-sec. intervals are shown in figure 14 by the short line segments crossing the aircraft track at right angles. The long segments indicate the subpoints at 10 sec. after each minute. The aircraft track, computed by integrating the ground velocity measured by the Doppler navigation system, is given by the dotted line on which the 10-, 30-, and 50-sec. positions of the aircraft are shown by one large and two small circles, respectively. The first photogrammetric and the Doppler positions at $15^h27^m10^s$ are assumed to be identical, and they are identified in the figure as the subpoint at 1527 EST+10 sec.

From these two subpoint tracks obtained by entirely different methods, the ground speed errors, $\Delta G/G$, were computed within 20-sec. sections of the subpoint track. The result presented in the upper chart of figure 15 suggests that the ground speed error averaged within each loop is very close to zero. The wild variation is a result of the inevitable error in the photogrammetric fixes at both ends of each track segment, about 1 mi. long.

The azimuths of the ground velocity obtained by the Doppler navigation system and by the photogrammetric fixes are compared. Their differences, obtained by subtracting the latter from the former, are presented in the lower chart of figure 15. The differences obviously represent $\Delta\delta+\Delta\zeta$, the sum of the drift-angle error and the compass heading error. The differences averaged over each complete loop are $-0.5°$ (1st), $-1.0°$ (2d), and $-2.5°$ (3d) loop, with a mean value of $-1.0°$, which is very close to $-0.87°$, the mean drift-angle error in table 3 obtained by an entirely different method.

## 9. DIVERGENCE AND VORTICITY COMPUTATION FROM LOOP FLIGHTS

Knowing that the errors $\Delta E$ and $\Delta\zeta$ can be determined with reasonable accuracy, we shall develop a method of computing divergence and vorticity inside a loop flown by an aircraft equipped with a Doppler wind system.

In order to simplify the problem, the wind direction and the speed within the loop are assumed to be more or less constant; and the plane flies along a circular track with respect to the coordinate system translating with the mean winds. As in the case of the error determination previously discussed, the wind speed is considered small in comparison with the true air speed of the aircraft.

Under this assumption, with the help of figure 16, we write the tangential and radial components of the measured winds at an arbitrary point on the circle thus:

$$W_t=W\cos\zeta+\Delta W\cos\zeta+W\Delta w\sin\zeta \tag{54}$$

$$W_r=W\sin\zeta+\Delta W\sin\zeta-W\Delta w\cos\zeta, \tag{55}$$

where $W_t$ and $W_r$ denote the tangential and radial components, respectively. By using the relationship expressed by equations (48) and (49), the above equations are reduced to

$$W_t=W\cos\zeta+\Delta E$$

$$W_r=W\sin\zeta-G\Delta\delta. \tag{57}$$

Then we integrate each component throughout the circumference and divide by the area of the circle. Thus we obtain

$$\text{Measured vorticity}=\frac{1}{\pi\rho^2}\int_0^{2\pi}W\cos\zeta d\theta+\frac{2}{\rho}\Delta E$$

$$=\text{True vorticity}+\frac{2}{\rho}\Delta E \tag{58}$$

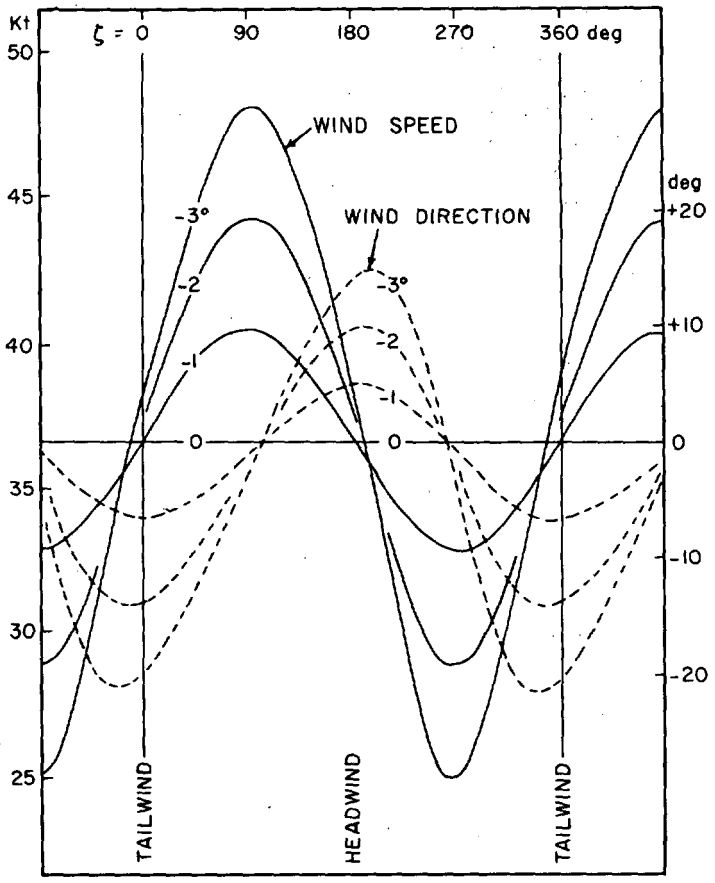


FIGURE 11.—Fluctuation of measured Doppler winds corresponding to the drift angle error at 1° intervals. The phases of the wind speed and direction fluctuations in this case lag 90° behind those caused by the true air speed, thus making it impossible to correct the drift angle error by changing the true air speed.

$$\text{Measured divergence}=\frac{1}{\pi\rho^2}\int_0^{2\pi}W\sin\zeta d\theta-\frac{2}{\rho}G\Delta\delta$$

$$=\text{True divergence}-\frac{2}{\rho}G\Delta\delta, \tag{59}$$

where $\theta$ is the angle measured from a reference direction through the center of the circle. These equations indicate that there exist inevitable errors in computing both divergence and vorticity from measured Doppler winds. It is feasible, however, to suppress these errors considerably by flying a loop with a relatively large diameter, since these errors are inversely proportional to the loop radius.

Shown in table 4 are such errors in divergence and vorticity when loops with various radii are flown. Both $\Delta E$ and $G\Delta\delta$ are assumed to be known to 1-kt. accuracy. It will be seen that these errors remain unchanged regardless of the flying speed, but the angle of bank determined by the speed and the diameter must always be kept below a ceiling of about 18° in order not to operate the Doppler system in a memory mode. For a 250-kt. aircraft speed, the minimum loop radius would be about 3 mi. When a

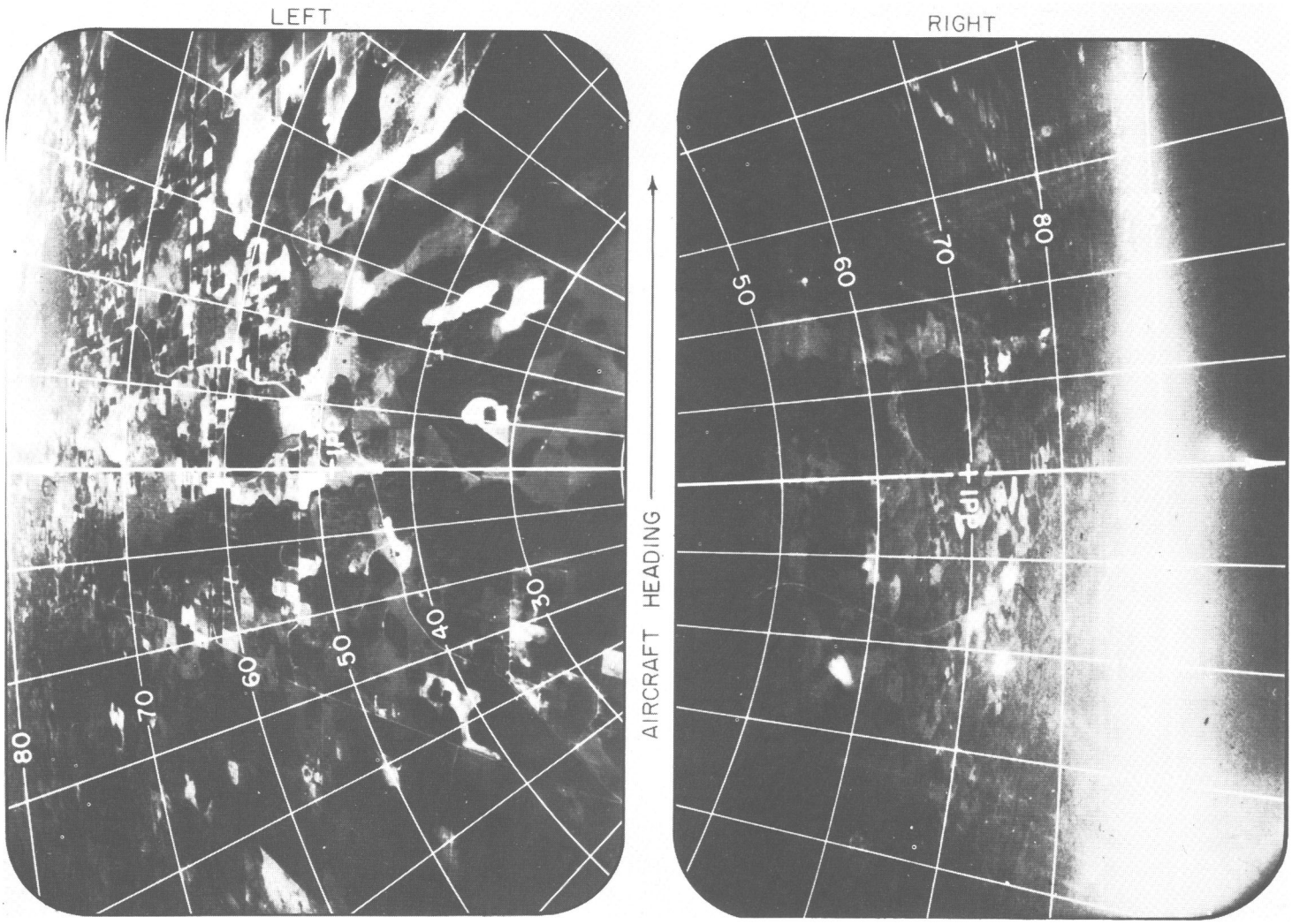


FIGURE 12.—Both right and left images taken by a pair of 35-mm. time-lapse cameras with 21-mm. lenses and double-frame advancement. The shutters are synchronized with the digital pulses so that the pictures are taken at 10, 30, 50 sec. of each minute. Superimposed on the pictures are the isolines of the nadir angles and the horizontal angles at 10° intervals.

jet aircraft with a 500-kt. speed is used, the minimum radius would increase to 15 mi., thus necessitating an 11-min. flight time for the completion of the loop.

Meteorological disturbances in an ordinary synoptic scale are characterized by divergence and vorticity of the order of $10^{-5}$ sec.$^{-1}$ In order to determine such a field of motion, based upon the 1-kt. accuracy of $\Delta E$ and $G\Delta\delta$, it would be necessary to fly a loop with a radius of 20 mi. or more. If an extremely large loop were flown, however, the wind field might change during the time required to complete such a loop.

TABLE 4.—*The vorticity and divergence errors when $\Delta E = G\Delta\delta = 1$ kt. Errors are tabulated as a function of the radius of loops flown by an aircraft. Aircraft speeds, 250 and 500 kt., are used in computing the angle of bank and the time required for a complete loop flight. When the bank reaches more than about 18°, Doppler systems usually operate in memory mode, thus restricting such a flight for wind computation purposes.*

| Loop radii, $\rho$ (n. mi.) | 3 | 5 | 10 | 15 | 20 | 25 | 30 |
|---|---|---|---|---|---|---|---|
| Errors in divergence and vorticity ($10^{-5}$ sec. $^{-1}$). | 18.8 | 11.2 | 5.6 | 3.7 | 2.8 | 2.2 | 1.9 |
| 250-kt. speed—Angle of bank (deg.) | 16.0 | 9.6 | 5.0 | 3.3 | 2.5 | 2.0 | 1.7 |
| 250-kt. speed—Time for loop (min.) | 5 | 7 | 15 | 22 | 30 | 38 | 45 |
| 500-kt. speed—Angle of bank (deg.) | (memory mode) | | | 14.5 | 10.0 | 7.9 | 7.1 |
| 500-kt. speed—Time for loop (min.) | (memory mode) | | | 11 | 15 | 19 | 22 |

So far we have assumed that both $\Delta E$ and $G\Delta\delta$ are known from equations (52) and (53) to the accuracy of 1 kt. It must be kept in mind that these equations were obtained under the assumption that a loop is flown in a non-divergent and irrotational wind field. Such an assumption is not always valid, thus necessitating the establishment of a method of determining $\Delta E$ and $G\Delta\delta$ while flying in a loop in a reasonably divergent and vortical wind field. By rearranging equations (58) and (59), we write

$$\frac{2}{\rho}\Delta E = \text{Measured vorticity} - \text{True vorticity} \qquad (60)$$

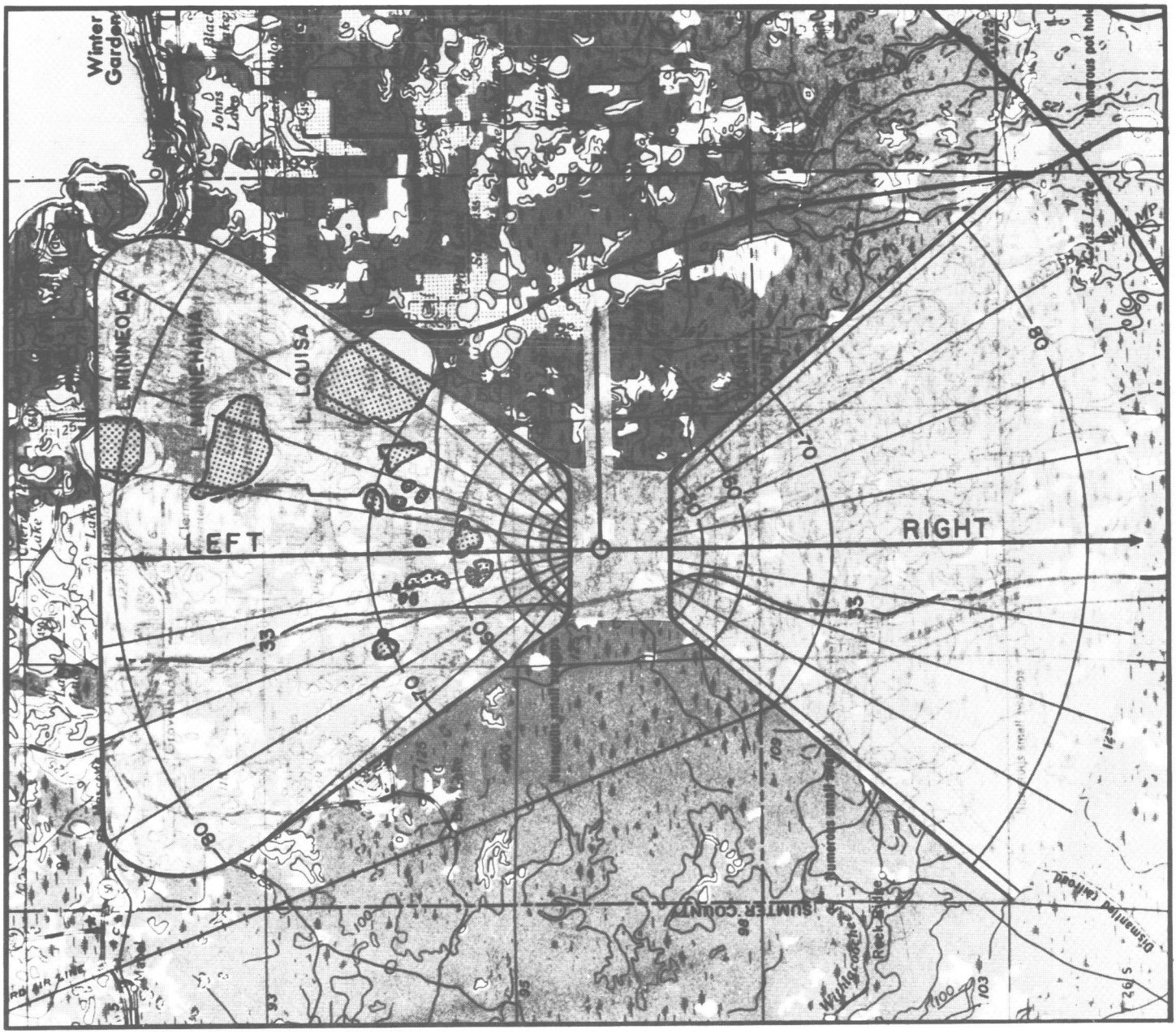


FIGURE 13.—Method of photogrammetric fixes of the aircraft locations. The rectified images, including significant landmarks, are first sketched in the fan-shaped areas representing the fields of view. These areas are then moved on a corresponding topographic map until the landmarks show the best possible agreement. The accuracy of the subpoint thus obtained is better than 0.1 mi.

and

$$-\frac{2}{\rho} G\Delta\delta = \text{Measured divergence} - \text{True divergence}. \quad (61)$$

These equations indicate that true values become insignificant compared with measured values as the loop radius decreases, because the values measured with a small loop are mostly those of errors. For example, a measured value obtained by a propeller aircraft flying around a 5-mi. loop would differ by $11\times10^{-5}$ sec.$^{-1}$ from the true value which is only a few tenths of this difference. Thus it is feasible to determine $\Delta E$ and $G\Delta\delta$ from equations (52) and (53) as long as the loop radius is kept reasonably small.

It may be concluded that large loops should be used for divergence and vorticity computation once Doppler speed and heading are calibrated by using data from small loops.

## 10. SUMMARY AND CONCLUSIONS

For the purpose of calculating true wind velocities from Doppler winds, two types of errors have been investigated.

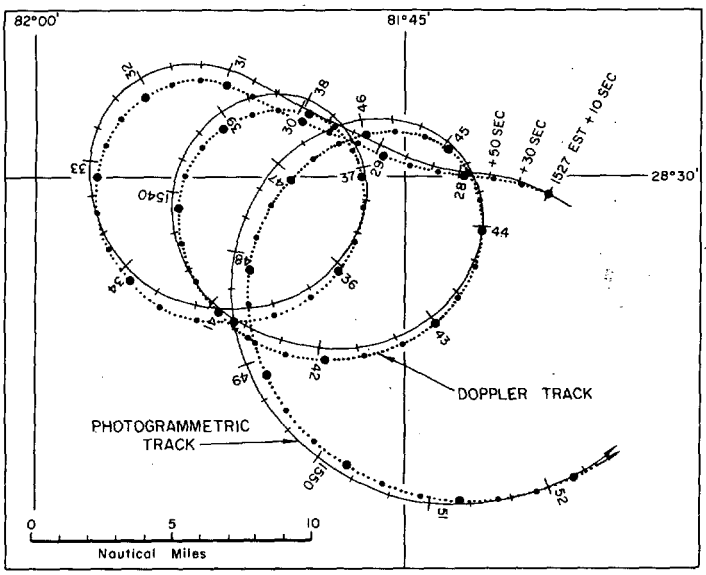


FIGURE 14.—Comparison of the photogrammetric positions indicated by the short lines intersecting the flight track, and the Doppler positions shown by the solid circle on the dotted flight track. The Doppler position at 1527 EST+10 sec. was brought to the photogrammetric position at the same time. Thereafter the positions at 10, 30, and 50 sec. of each minute were computed. From Florida test flight of November 6, 1963.

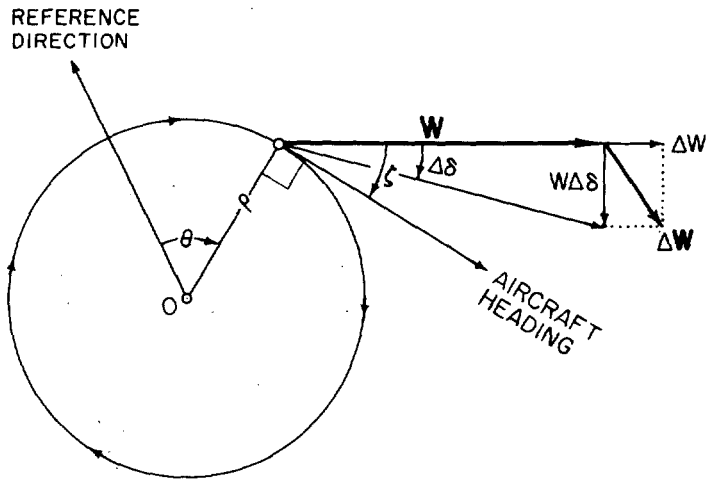


FIGURE 16.—Geometry to compute divergence and convergence from the Doppler winds measured along a circular flight track on the relative coordinates moving with the winds. The Doppler winds are assumed to include a small error of ΔW expressed as a vector. The reference direction of the angle $\theta$ is arbitrary.

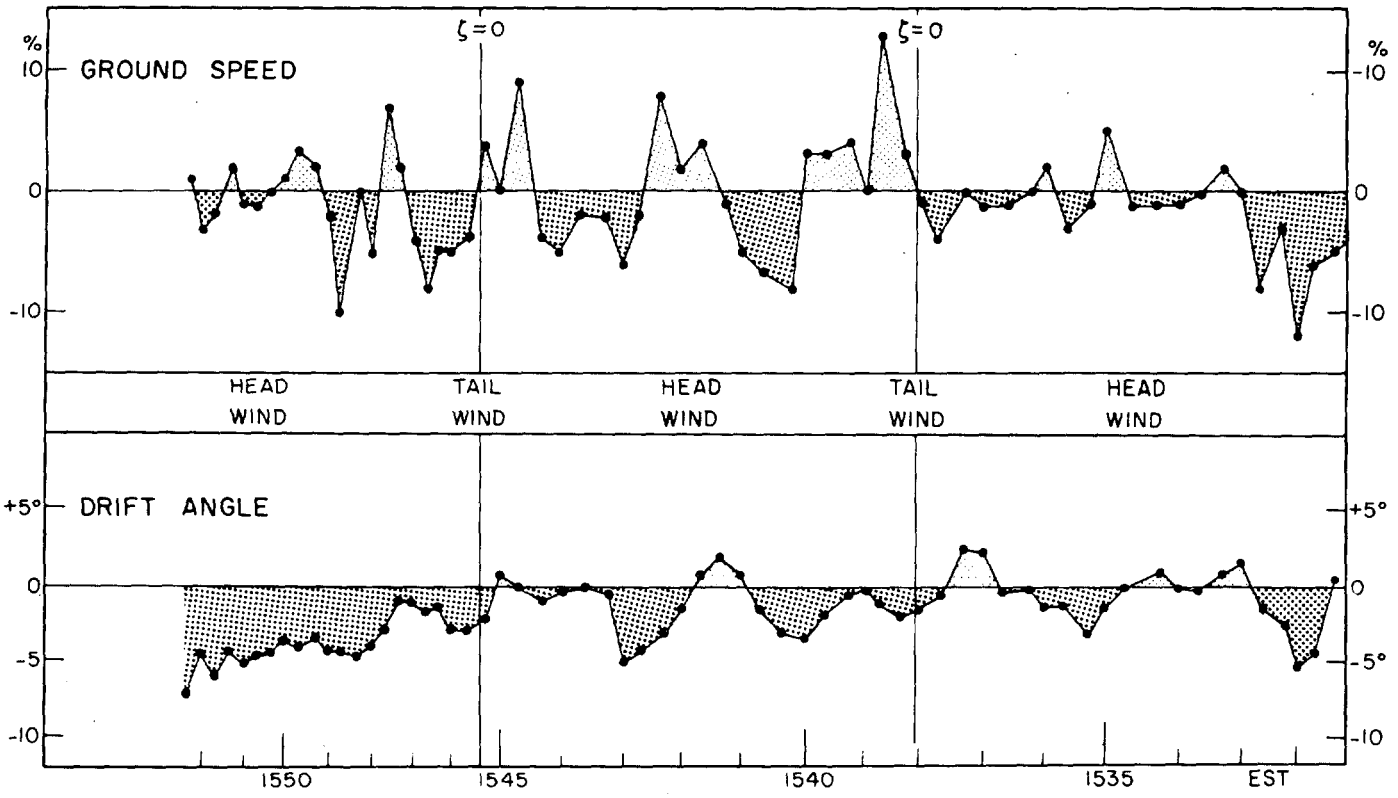


FIGURE 15.—The difference between the Doppler ground speed and the photogrammetric ground speed expressed in the fraction of the latter (upper), and that between the directions of the ground velocities by Doppler and photogrammetric methods (lower). From Florida test flight of November 6, 1963.

The first type, which is instrumental in nature, is caused by the calibration error in the ground speed and the true air speed and also by misalignment of the Doppler antennas. Since errors of this type are usually very small, the true winds can be calculated after applying corrections to the drift angle and to the true air speed. It was found that the exact amounts of correction can be calculated from the Doppler winds measured while flying along a complete loop. In order to minimize the influence of the vortical and divergent wind field in which an aircraft flies, the loop radius should be kept small without throwing the Doppler operation into memory mode. Such a loop flight can be completed in about 5 min. by a propeller plane and in about 10 min. by a jet.

Detailed analysis of two test flights using a U.S. Weather Bureau DC–6B aircraft over Florida and Oklahoma revealed that the drift-angle and the true air speed can be calibrated with accuracies of about 0.2° and 1 kt., respectively. These accuracies will permit us to calculate true wind velocity with vector errors less than 2 kt.

When one or more Doppler beams is under the influence of moving water particles, the second type of wind error must be taken into account. Theoretical errors were obtained under the assumption that some or all four Doppler beams obtain return signals from particles in motion relative to the ground. It was found that the fall velocities of raindrops do not alter the Doppler velocity if their effective velocities are uniform for all beams. If flights are made over a non-uniform velocity field, this alters not only the Doppler speed but also the Doppler heading.

Influences of horizontal velocities of moving water particles were studied theoretically, leading to the establishment of a Doppler triangle. This triangle is constructed as a function of effective velocities influencing each of the Doppler beams. The present study revealed that the Doppler heading is perpendicular to the base of the triangle and that the Doppler speed is the triangle's altitude multiplied by a constant.

This simple procedure can be widely used in estimating possible errors in Doppler winds when the effective velocities of precipitating echoes are known. If the effective velocities are not known, however, it is feasible to determine them. By flying along a coast line, for instance, a pilot can maneuver the aircraft so that no beams, two beams, and four beams repeatedly lock over the water. The periodic change in Doppler winds thus obtained permits us to determine the coastal current if it exceeds a few knots. Another interesting experiment is that of wind measurement while keeping only one beam wet. The wind error in this experiment should be zero if an aircraft approaches an echo from a particular direction. On the other hand, the error would reach the maximum when the direction of approach is changed by 90°. The vector difference between these Doppler winds permits us to determine the effective velocity of the precipitation.

It is expected that the results presented in this paper will be used in designing specific flight patterns for the purpose of studying mesoscale wind fields associated with small cumulus to more vigorous convection systems such as thunderstorms and hurricane rainbands.

## ACKNOWLEDGMENTS

The author is very grateful to the staff members of the Satellite and Mesometeorology Research Project of the University of Chicago, especially Messrs. Frank Norimoto and James E. Arnold for their participation in the research loop flights over Florida and Oklahoma and Robbi Stuhmer who made photogrammetric analyses of aerial photographs taken during the test flights. Sincere appreciation should be expressed to the staff members of the Research Flight Facility, U.S. Weather Bureau, who performed successful loop flights for the purpose of evaluating the performance of the Weather Bureau's DC–6B's, and especially to Mr. Harlan Davis for his valuable suggestions and technical information with regard to the Weather Bureau's Doppler wind systems.

## REFERENCES

1. A. B. Arnett, "Anomalous Wind Field in the Immediate Environments of Two Severe Thunderstorms as Observed by Aircraft," *Proceedings of the Second Annual Conference on Weather Effects on Aircraft Systems*, Trenton, N.J., 1962, pp. 71–80.
2. F. B. Berger, "Design of Airborne Doppler Velocity Measuring Systems," vols. 1 and 2, *Technical Series GPL Division*, General Precision, Inc., Pleasantville, N.Y., 1957.
3. T. Fujita, "A Technique for Precise Analysis of Satellite Data, Vol. I—Photogrammetry," *Meteorological Satellite Laboratory Report* No. 14, U.S. Weather Bureau, 1963, 106 pp.
4. T. Fujita and J. E. Arnold, "Development of a Cumulonimbus Under the Influence of Strong Vertical Wind Shear," *Proceedings, 10th Weather Radar Conference*, 1963, pp. 178–186.
5. C. R. Grant and B. S. Yaplee, "Backscattering from Water and Land at Centimeter and Millimeter Wavelengths," *Proceedings of the I.R.E.* vol. 45, 1957, pp. 976–982.
6. N. E. LaSeur and H. F. Hawkins, Jr., "An Analyisis of Hurricane Cleo (1958) Based on Data from Research Reconnaissance Aircraft," *Monthly Weather Review*, vol. 91, Nos. 9–12, Sept.–Dec. 1963, pp. 694–709.
7. G. S. McLean, "Observation of Severe Convective Activity in a Squall Line," *Bulletin of the American Meteorological Society*, vol. 42, No. 4, Apr. 1961, pp. 252–264.
8. Research Flight Facility, *Manual of Meteorological Instrumentation and Data Processing*, U.S. Weather Bureau, 1964.
9. R. H. Simpson, "Structure of an Immature Hurricane," *Bulletin of the American Meteorological Society*, vol. 35, No. 8, Oct. 1954 pp. 335–350.
10. J. C. Wiltse, S. P. Schlesinger, and C. M. Johnson, "Backscattering Characteristics of the Sea in the Region from 10 to 50 KMC," *Proceedings of the I.R.E.*, vol. 45, 1957, pp. 220–228.

[*Received August 10, 1965; revised October 18, 1965*]